

L. C. Demartini, H. A. Vielmo  
and S. V. Möller

Universidade Federal do Rio Grande do Sul  
Programa de Pós-Graduação em  
Engenharia Mecânica  
Rua Sarmento Leite, 425  
90050-170 Porto Alegre, RS, Brazil  
vielmoh@mecanica.ufrgs.br  
svmoller@vortex.ufrgs.br

# Numeric and Experimental Analysis of the Turbulent Flow through a Channel With Baffle Plates

*The present work presents the numeric and experimental analysis of the turbulent flow of air inside a channel of rectangular section, containing two rectangular baffle plates. This is an important problem in the scope of heat exchangers where the characterization of the flow, pressure distribution, as well as the existence and the extension of possible recirculations need to be identified. The differential equations that describe the flow were integrated by the Finite Volumes Method, in two dimensions, employing the Fluent software with the k-ε model to describe the turbulence. The mesh is structured, with rectangular volumes. Several boundary conditions were explored, being the more realistic results obtained by prescribing the inlet velocity field and atmospheric pressure at the exit. The obtained results are compared with experimental data, being analyzed and commented the deviations. The velocity field was measured with a hot wire anemometer, and the pressure field with an electronic manometer. The largest variations in the pressure and velocity fields occur in the regions near to the deflectors, as expected.*

**Keywords:** Numerical simulation, experimental simulation, turbulence, fluent, hot wires

## Introduction

Banks of tubes are found in many industrial processes and in the nuclear industry, being the most common geometry used in heat exchangers. The heat is transferred from the fluid inside the tubes, to the turbulent flow outside them. Usually, a very complex flow is found there, where besides the turbulence, boundary layer separation and recirculating flows are found in the external flow.

In shell-and-tube heat exchangers, the cross flow through the banks is obtained by means of baffle plates, responsible for changing the direction of the flow and for increasing the heat exchange time between fluid and the heated surfaces. Baffles have also the purpose of increasing turbulence levels and, thus, heat exchange ratios (Nusselt number - Nu). On the other side, boundary layer separation after the baffles may occur, as demonstrated in the old, but still very interesting results of flow visualization in models of heat exchangers and steam generators by Wiemer, 1937. This can be an additional and important source of disturbances in the flow, which can travel through the bank, influencing the tube bank and the baffles.

Experimental results of velocity and wall pressure fluctuations in the turbulent flow through a simulated tube bank with square arrangement, after passing a baffle plate were performed by Möller et al., 1999. In general, results of wall pressure and wall pressure fluctuations showed higher values than in pure cross flow (Endres, 1997; Endres & Möller, 2001). The characteristic value of the Strouhal number found was about 0.2. Important additional peak frequencies, appearing in spectra of tube wall pressure fluctuation, could not be associated neither to effects of pure cross flow through the bank nor to effects produced solely by the baffles.

Baffle plates and obstacles submitted to laminar and turbulent flows has being analyzed in the recent years by several authors, using numerical and/or experimental techniques.

Numerical analysis of the laminar flow with heat transfer between parallel plates with baffles was performed by Kelkar and Patankar, 1987. Results show that the flow is characterized by strong deformations and large recirculation regions. In general, Nusselt number and friction coefficient (fR) increase with the Reynolds number.

Hwang et al., 1999, simulated the turbulent flow impinging on an obstacle using a two-dimensional k-ε model. Numerical results show that the extension of the recirculation region upstream of the obstacle does not depend on its length in flow direction. This does not happen in the region downstream of the obstacle, where the recirculation is strongly influenced by the length of the obstacle, decreasing when obstacle length is increased, but remaining constant when the flow on the upper side of the obstacle reattaches.

De Zilwa et al., 1998, studied laminar and turbulent flows through plane sudden-expansions. Turbulent flow simulations using k-ε models showed to be very reliable when compared to experimental results, except near the walls in the recirculation regions, underestimating the reattachment location.

Measurements using LDA technique in the turbulent flow in a duct with several baffle plates were performed by Berner et al., 1984, with the purpose of determining the number of baffles necessary for obtaining a periodic boundary condition and the dependence on Reynolds number and the geometry. Results showed that with a Reynolds number of  $5.17 \times 10^3$ , four baffles are necessary for obtaining a periodic boundary condition. By increasing the Reynolds number to  $1.02 \times 10^4$ , a periodic boundary condition is obtained with three baffles.

Antoniu and Bergeles, 1988, analyzed the flow over prisms with several aspect ratios using hot wire technique. By increasing the aspect ratio L/H, the flow reattaches on the prism surface and downstream, while recirculation lengths and turbulence scales are reduced.

Characteristics of the turbulent flow with heat transfer in a rectangular duct with baffle plates were studied by Habib et al., 1994. The heat flux was uniform in both upper and lower walls. The experiment focused on the influence of Reynolds number and baffle height on the local and global heat transfer coefficients, and pressure drop measurements.

Large recirculation regions and velocity gradients were observed behind the baffles. Pressure drop increases more rapidly than the heat transfer coefficient with the Reynolds number.

Li and Kottke, 1998, studied heat transfer and pressure drop in simulating models of shell-and-tube heat exchangers. Parameters of the experimental work were the Reynolds number and the distance between the baffles. Results demonstrated that for a constant value of the Reynolds number, increasing the distance between the baffles increased the heat exchange coefficient and the pressure drop.

Behavior of the turbulent flow and the heat transfer on obstacles was also studied by Acharya et al.,1998, using k-ε model and experimental techniques.

The purpose of the present work is to investigate the turbulent flow of air inside a channel of rectangular section, containing two rectangular baffle plates as presented in more detail in Demartini (2001). The characterization of the flow field in this channel intend to allow the comprehension of the behavior of dynamic loads, produced by the fluctuating velocity and pressure fields, and contributes to the characterization of heat transfer distribution in heat exchangers. Hot wire anemometry and the Finite Volume Method, by means of commercial program Fluent 5.2 (© Fluent Inc., 2000), are applied in this research work.

### Test Section and Experimental Procedure

The test section, shown in Fig.1, is a 1370 mm long rectangular channel, with 146 mm height and a width of 193 mm. This is the same test section described in Möller at al.,1999, and Endres and Möller, 2001, but the tube bank was removed, to allow the study of the flow on the baffle plates. Air is the working fluid, driven by a centrifugal blower, passed by a settling chamber and a set of honeycombs and screens, before reaching the baffle plates with about 2 % turbulence intensity. Two baffle plates were placed on opposite channel walls. The flow rate, and thus the Reynolds number, was controlled by a gate valve. Before the tube bank a Pitot tube was placed, at a fixed position to measure the reference velocity for the experiments.

Mean wall pressure and dynamic pressure from the Pitot tube were measured by means of H&B ARA 500 pressure transmitters. Pressure measurements were performed at the side wall of the channel.

The Reynolds number, calculated with the hydraulic diameter of the channel and the reference velocity is  $Re = 8.73 \times 10^4$ . This velocity was determined with help of the fixed Pitot tube, as described above.

Velocity and velocity fluctuations were measured by means of a DANTEC *StreamLine* constant temperature hot wire anemometer. Previous analysis of the behavior of the test section, by means of METRA accelerometers, and of the measurement technique, allowed to identify peaks in spectra due to resonances not related to the phenomena investigated. Data acquisition of velocity fluctuations was performed simultaneously by a 12-bit Keithley DAS-58 A/D-converter board, controlled by a personal computer, which was also used for the evaluation of the results.

For the determination of autospectral density functions, the sampling frequency was of 5 kHz, while the signals of the instruments were high pass filtered at 1 Hz, and low pass filtered at 2 kHz, to avoid effect of folding of frequencies higher than the cut off (Nyquist) frequency. Previous studies of pure cross flow through tube banks showed, for this test sections, to be the frequency range of importance (Endres and Möller, 2001).

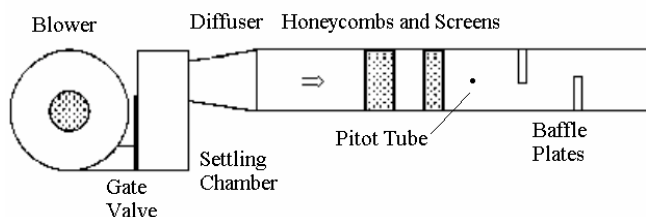


Figure 1. Schematic view of the test section. Flow from left to right.

### Presentation of the Problem Studied and its Numerical Approach

In this Chapter balance equations and the method employed to the solution of the problem investigated, including the necessary simplifications, are described.

### Turbulence Modelling

Reynolds-Averaged Navier-Stokes Equations are the governing equations for the problem analyzed (momentum balance), with the continuity equation. For a two-dimensional incompressible flow of a newtonian fluid, mass and momentum equation become, respectively

$$\frac{\partial \bar{U}_j}{\partial X_j} = 0, \quad (1)$$

and

$$\rho \bar{U}_j \frac{\partial \bar{U}_i}{\partial X_j} = -\frac{\partial \bar{p}}{\partial X_i} + \frac{\partial}{\partial X_j} \left( \mu \frac{\partial \bar{U}_i}{\partial X_j} - \rho \overline{U_i U_j} \right), \quad (2)$$

where  $\rho$  is the fluid density (constant),  $p$  the pressure,  $\mu$  dynamic viscosity,  $\bar{U}_i$  and  $\bar{U}_j$  are mean velocity components in  $X_i$  and  $X_j$  directions.

In eq. (2),  $\rho \overline{U_i U_j}$  is the additional term of Reynolds stresses due to velocity fluctuations, which has to be modeled for the closure of Eq. (2). The classical approach is the use of Boussinesq hypothesis, relating Reynolds stresses and mean flow strain, through the eddy viscosity concept [Hinze, 1975]. In its general formulation, as proposed by Kolmogorov, Boussinesq hypothesis is written as

$$-\rho \overline{U_i U_j} = \mu_t \left( \frac{\partial \bar{U}_i}{\partial X_j} + \frac{\partial \bar{U}_j}{\partial X_i} \right) - \frac{2}{3} \rho \delta_{ij} k, \quad (3)$$

where  $\mu_t$  is the eddy viscosity,  $\delta_{ij}$  the Kroencker Delta and  $k$  the kinetic energy of the turbulence, defined as:

$$k = \frac{1}{2} \overline{U_i U_i}. \quad (4)$$

Successful turbulence models are those based on the eddy viscosity concept, which solve two scalar transport differential equations. The most well known is the k-ε model [Lauder and Spalding, 1972].

The so called "standard" k-ε model is a semi-empirical one, based on the conservation equation of the kinetic energy ( $k$ ) and its dissipation rate ( $\epsilon$ ). The basis of the model is the Boussinesq's hypothesis, that the Reynolds stresses  $-\rho \overline{U_i U_j}$  are proportional to the strain rate of the mean flow, by means of the eddy viscosity concept, thus

$$\mu_t = \rho C_\mu \frac{k^2}{\epsilon}. \quad (5)$$

Balance equations for the kinetic energy ( $k$ ) and its dissipation rate ( $\epsilon$ ) for the model are, respectively

$$\rho \left( \frac{\partial k}{\partial t} + U_j \frac{\partial k}{\partial X_j} \right) = \frac{\partial}{\partial X_j} \left[ \left( \mu + \frac{\mu_t}{\sigma_k} \right) \frac{\partial k}{\partial X_j} \right] + G_k - \rho \varepsilon, \quad (6)$$

$$\rho \left( \frac{\partial \varepsilon}{\partial t} + U_j \frac{\partial \varepsilon}{\partial X_j} \right) = \frac{\partial}{\partial X_j} \left[ \left( \mu + \frac{\mu_t}{\sigma_\varepsilon} \right) \frac{\partial \varepsilon}{\partial X_j} \right] + C_{1\varepsilon} \frac{\varepsilon}{k} G_k - C_{2\varepsilon} \rho \frac{\varepsilon^2}{k}, \quad (7)$$

where:

$$C_\mu = 0,09; \quad C_{1\varepsilon} = 1,44; \quad C_{2\varepsilon} = 1,92; \quad \sigma_k = 1,0; \quad \sigma_\varepsilon = 1,3,$$

are the constants of the model.

In Eqs. (6) and (7),  $G_k$  represents the production rate of the kinetic energy due to the energy transfer from the mean flow to turbulence, given by

$$G_k = -\rho \overline{U_i U_j} \frac{\partial \overline{U_j}}{\partial X_i}. \quad (8)$$

The production term  $G_k$  is modeled according to Boussinesq's hypothesis, by:

$$G_k = \mu_t S^2, \quad (9)$$

where  $S$  is the modulus of the mean strain tensor, given by

$$S = \sqrt{2S_{ij}S_{ij}}, \quad (10)$$

and the strain tensor is

$$S_{ij} = \frac{1}{2} \left( \frac{\partial \overline{U_i}}{\partial X_j} + \frac{\partial \overline{U_j}}{\partial X_i} \right), \quad (11)'$$

which is the symmetrical part of the velocity gradient.

The presence of a wall influences the velocity field in its vicinity through the non slip boundary condition. Considering the effects of the wall for the standard  $k-\varepsilon$  model, based on Launder and Spalding, 1974, a "law of the wall" for the mean velocity distribution is given by

$$U^* = \frac{1}{\kappa} \ln(Ey^*), \quad (12)$$

where  $y^*$  is the dimensionless distance to the wall is given by:

$$y^* = \frac{\rho C_\mu^{1/4} k_p^{1/2} y_p}{\mu}, \quad (13)$$

and:

$\kappa$  = von Kármán constant (= 0.42)

$E$  = empirical constant (= 9,81)

$\overline{U}_p$  = time average velocity at position  $P$

$k_p$  = kinetic energy of turbulence at position  $P$

$y_p$  = distance from position  $P$  to the wall

## Problem Definition and Boundary Conditions

The problem to be analyzed is the turbulent flow in a rectangular cross section duct where two baffles were placed, so as to simulate the conditions found in shell-and-tube heat exchangers, where flow and pressure distribution need to be known. A schematic view of the physical problem is shown in Fig.2.

The Reynolds number of the experiments is  $Re = 8.73 \times 10^4$ , defined as

$$Re = \frac{\rho D_H U_0}{\mu}, \quad (14)$$

where  $U_0$  is the entrance (reference) velocity, 7.8 m/s, and  $D_H$  is the hydraulic diameter of the channel, equal to 0.167 m.

The total length of the channel is equivalent to 3.307 hydraulic diameter, which is not sufficient for the flow development. Therefore, no influence will result from the side walls, so that the flow can be considered as being two-dimensional. Previous measurements of the flow velocity distribution in the outlet of the channel without any obstacle showed the validity of this hypothesis.

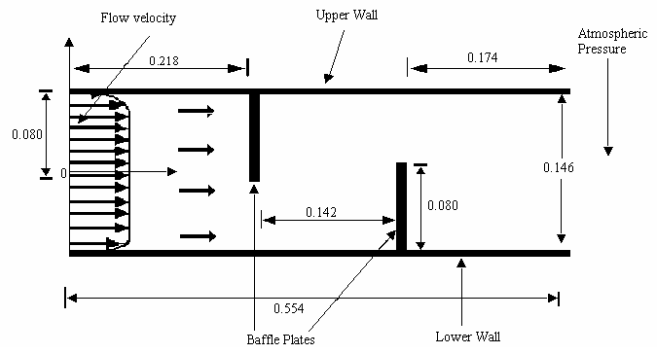


Figure 2. Detail of the test section with the baffle plates and boundary conditions (dimensions in m).

In the entrance region, a velocity profile was prescribed, as shown in Fig. 2. This velocity profile was obtained by means of hot-wire measurements. Kinetic energy of turbulence and dissipation rates are prescribed, respectively, as

$$k_\circ = 0,005U_0^2, \quad (15)$$

and

$$\varepsilon_\circ = 0,1k_\circ^2. \quad (16)$$

For the upper and lower walls it is imposed

$$\frac{\partial k}{\partial n} = 0, \quad (17)$$

for the kinetic energy, where  $n$  is the coordinate normal to the wall, and  $\varepsilon$  is computed in the volume  $P$  adjacent to the wall as,

$$\varepsilon_p = \frac{C_\mu^{3/4} k_p^{3/2}}{\kappa y_p}. \quad (18)$$

Besides, non slip and impermeability boundary conditions are imposed at the walls. In the channel outlet it is prescribed the atmospheric pressure.

## Numerical Method

Differential equations were integrated through the Finite Volume Method, using a two-dimensional formulation with the SIMPLEX-algorithm (van Doormaal, Raithby, 1985) for pressure-velocity coupling. Structured meshes, with rectangular volumes were built and tested with the Fluent 5.2 (©Fluent Inc., 2000).

Considering the characteristics of the flow, the Quick-scheme was applied to the interpolations (Leonard, Mokhtari, 1990), while a second-order upwind scheme was used for the pressure terms.

The mesh was generated by the pre-processor software Gambit 1.0. The mesh was refined at all solid boundaries, with volumes growing in geometrical progression with the increasing distance from the wall, as given by the expression

$$a_n = a_1(q^{n-1}), \quad (19)$$

where  $a_n$  is the length of the last volume from the wall,  $a_1$  is the length of the first volume adjacent to the wall,  $q$  is the growth ratio and  $n$  is the number of volumes. This expression is valid for the regions near the walls. For the regions more distant from the walls, the mesh is uniform, as a first tentative.

After importing the mesh from the preprocessor, additional refinements were performed, considering the geometry and features of the numerical solution of the problem. Figure 3 presents an example of the mesh used near the tip of a baffle plate, in the presence of flow separation. The mesh is too fine near the solid boundary so that graphic representation is beyond printer resolution. This refinement was necessary to resolve the strong velocity and pressure gradients in that region.

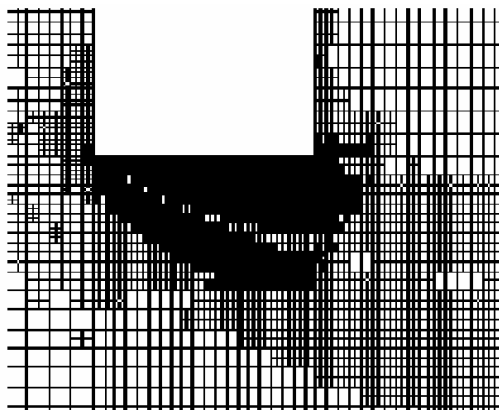


Figure 3. Mesh generated on the tip of the first baffle plate with refinements near the solid boundary to resolve velocity and pressure gradients.

## Results

Numerical results of mean velocity profiles for positions  $x = 0.159$  m and  $x = 0.189$  m, measured downstream of the entrance, are shown in Fig. 4. These positions are located upstream of the first baffle plate, located at a  $x = 0.218$  m from the entrance. Velocity values are scaled to the velocity at the entrance (reference velocity). The influence of the deformation of the flow field increases as the flow approaches the first baffle plate, increasing the velocity of the flow approaching the passage under the baffle.

Between the baffles, at locations  $x = 0.255$  m and  $x = 0.285$  m from entrance, respectively 0.027 and 0.057 m after the first baffle plate, the flow is characterized by very high velocities at the lower part of the channel, approaching 250 % of the reference velocity, which is 7.80 m/s, as shown in Fig. 5. In the upper part of the

channel, negative velocities indicate the presence of recirculation behind the first baffle.

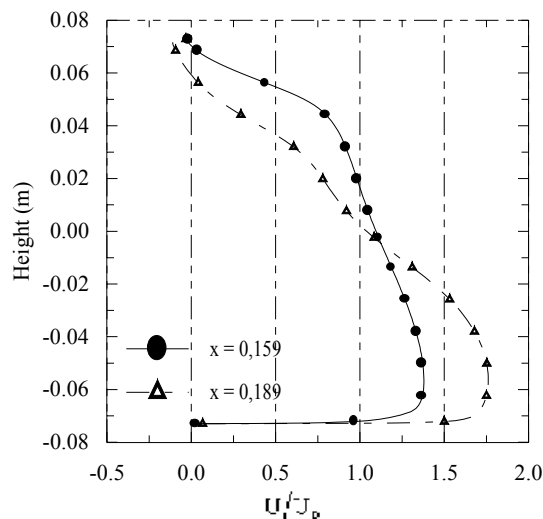


Figure 4. Dimensionless velocity profiles upstream of the first baffle plate.

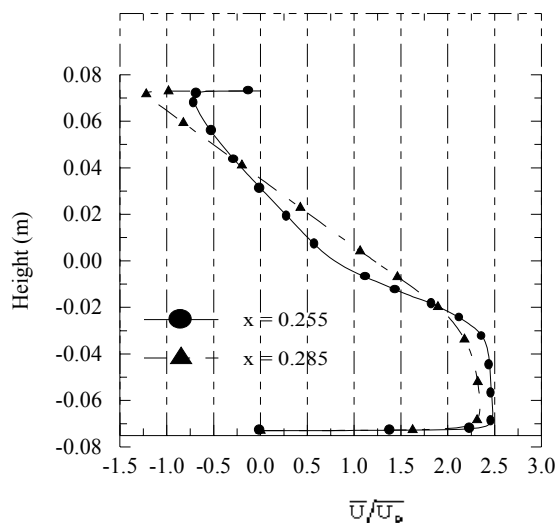


Figure 5. Dimensionless velocity profiles between the first and the second baffle plates.

Figure 6 shows the dimensionless velocity profiles at positions given by  $x = 0.315$  m and  $x = 0.345$  m, 0.055 m and 0.025 m before the second baffle plate. In these locations, results show that as the flow approaches the second baffle, its velocity is reduced in the lower part of the channel, while in the upper part is increased. Negative values observed in the numerical results from location  $x = 0.315$  m disappear at  $x = 0.345$  m, and the velocity profile is almost flat in the lower part of the channel, while in the upper part the flow starts to accelerate toward the gap above the second baffle plate.

A comparison of numerical and experimental results of velocity profiles after the second baffle plate, near the channel outlet is given in Fig. 7. At a position  $x = 0.525$  m, 29 mm before channel outlet, the value of the velocity reaches 34 m/s, 4.36 times higher than the entrance (reference) velocity. These values are only possible due to the very strong flow recirculation on the back side of the second baffle plate, which leads air from outside of the channel into the test section. The strong velocity variation from negative to positive

values could not be resolved by the relatively coarse experimental data mesh in that region, but the numerical results helped the analysis of the experimental results, since hot wires are not sensitive to changes in the velocity direction, confirmed by Pitot tube measurements.

The presence of the baffle plates influences not only the velocity field but also the pressure distribution in the whole domain investigated. To represent the pressure field in dimensionless form, a pressure coefficient is defined as

$$C_p = \frac{(p - p_{atm})}{\frac{\rho U_0^2}{2}}, \quad (20)$$

where  $p$  is the static pressure and  $p_{atm}$  is the atmospheric pressure. For the comparison of numeric with experimental results of  $C_p$ , the pressure  $p$  is the measured wall pressure or the calculated pressure.

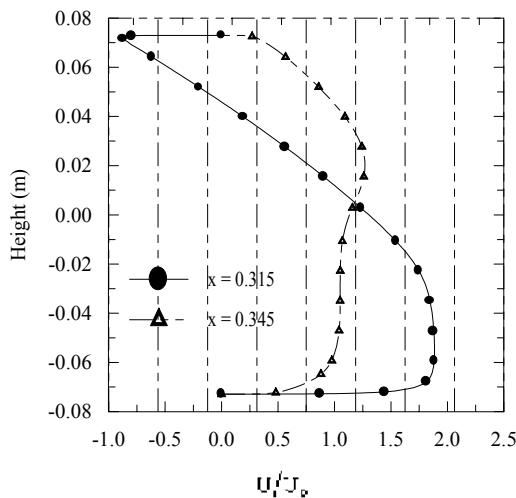


Figure 6. Dimensionless velocity profile upstream of the second baffle plate.

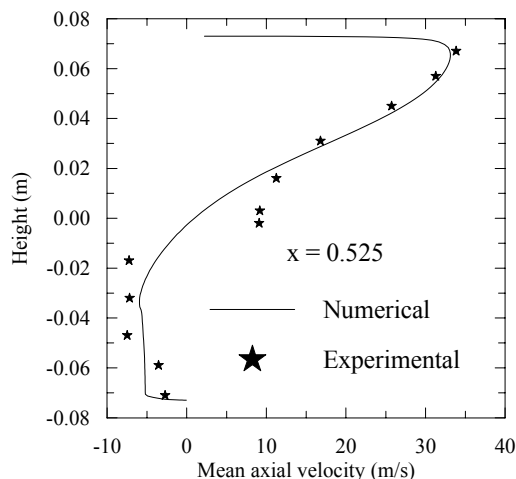


Figure 7. Comparison of numerical and experimental velocity profiles after the second baffle plate, near the channel outlet.

Figure 8 shows the magnitude of the velocity field. Numerical results show very low velocity values adjacent to the baffle plates. In the regions downstream of both baffle plates, recirculation cells with very low velocity values are observed. In the regions between the tip of the baffle plates and the channel walls, the velocity is

increased. Due to the changes in the flow direction produced by the baffle plates, the highest velocity values appear near the upper channel wall with an acceleration process that starts just after the second baffle plate.

Figure 9 shows numerical and experimental results of the pressure coefficient in positions at  $x = 0.189$  m and  $x = 0.255$  m, respectively 0.029 m before and 0.027 m after the first baffle plate. The greatest values occur, as expected, upstream of the considered baffle. In both cases elliptic influence of the baffles is observed. Firstly, by the growth of pressure coefficient for  $x = 0.189$  m, in the upper part of the channel and, secondly, downstream of the baffle in the lower part of the channel. The latter is produced by the presence of the second baffle.

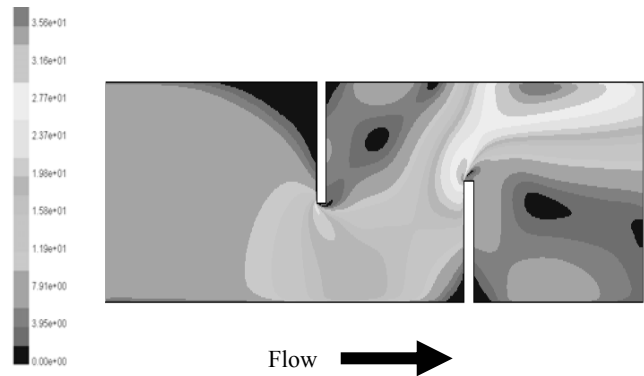


Figure 8. Velocity field distribution. Flow is from left to right. Velocity values in m/s.

Numerical results of pressure coefficients at positions  $x = 0.345$  m and  $x = 0.405$  m, respectively 0.025 m before and after the second baffle plate, are shown in Fig. 10, together with the corresponding experimental results. Similarly to the results in Fig. 9, the largest variations are found near the tip of the baffle, due to the strong velocity gradients in that region.

Downstream of the considered baffle plate, pressure coefficients present negative values, meaning that the pressure in that location is below atmospheric pressure. This fact is associated to the negative velocities at the channel outlet shown in Fig. 7.

Figures 11 and 12 show the distribution of the pressure coefficient in the lines starting from the tip of the baffles to the opposite walls. Pressure measurements were performed at the sidewall of the channel. Figure 11 shows experimental and numerical results under the first baffle, while Fig. 12 shows the results above the second baffle. In general, a good agreement between numerical and experimental results is observed showing the growth of the pressure coefficient near the walls. The lower pressure values near the tip of the baffles are due to the high velocities in that region.

### Concluding Remarks

Baffle plates play an important role in the dynamics of the flow through shell-and-tube heat exchangers. For the better comprehension of the phenomena produced by these devices, the search of detailed informations about the flow characteristics is necessary.

In this paper, the flow through a rectangular channel, where two baffle plates were placed in opposite walls, is studied. The geometry of the problem is a simplification of the geometry of baffle plates found in shell-and-tube heat exchangers. A commercial software (Fluent 5.2, © Fluent Inc., 2000), and hot wire anemometry were applied for the solution of the problem.

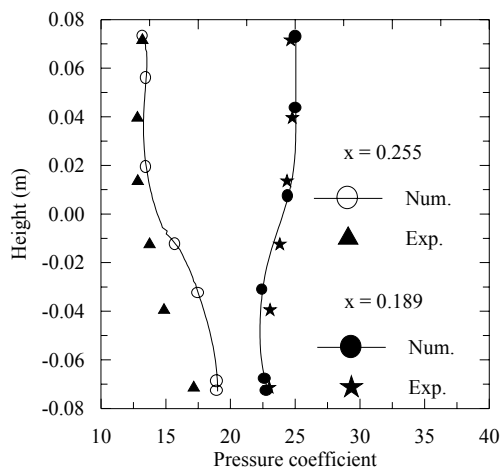


Figure 9. Comparison of numerical results of the pressure coefficient upstream and downstream of the first baffle plate with experimental results measured at the channel wall.

In general, the results found in this research work explain the unexpected results in a tube bank mounted in the same baffle plate channel (Möller et al., 1999), since there, the extension of the recirculation regions could not be properly considered.

The most important features observed are the high pressure regions formed upstream of both baffle plates, and the extent of the low pressure regions on the downstream regions. The latter are strongly associated with the boundary layer separation on the tip of the baffle plates, which is also influenced by the thickness of the baffle plates, in accordance with the results by Hwang et al., 1999.

Low and high pressure regions are associated to recirculation regions. The most intense is that occurring downstream of the second baffle plate, responsible for the high flow velocities observed at the outlet of the test section, creating a negative velocity profile which introduces mass inside the test section through the outlet.

Experiment and numerical analysis complement each other to perform the proposed study in this paper. While experiment provided the necessary boundary conditions and the results for evaluation and comparison of the numerical results, the computer code enlightened the flow distribution, the interpretation of the hot wire results, of the pressure field and the extension of the recirculation regions.

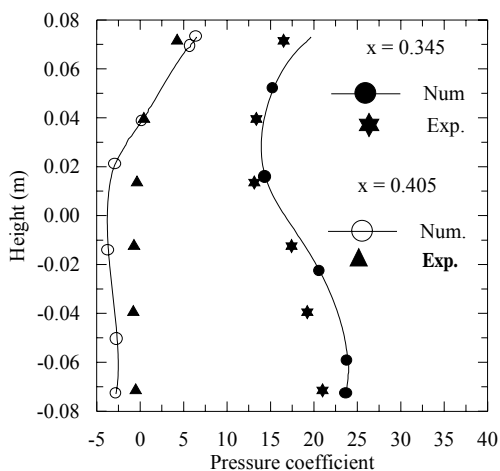


Figure 10. Comparison of numerical results of the pressure coefficient upstream and downstream of the second baffle plate with experimental results measured at the channel wall.

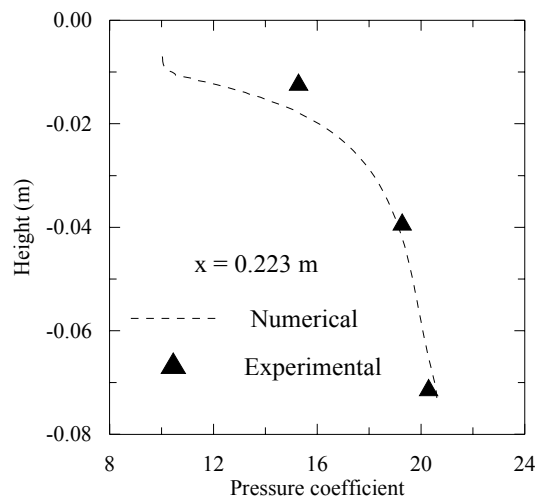


Figure 11. Comparison of numerical results of the pressure coefficient under the first baffle plate with experimental results measured at the channel wall.

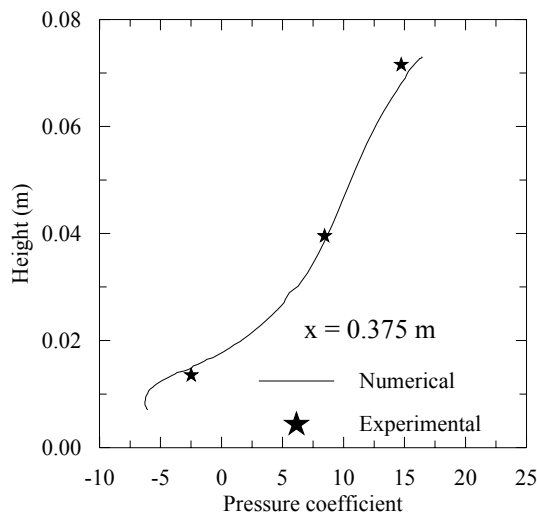


Figure 12. Comparison of numerical results of the pressure coefficient above the second baffle plate with experimental results measured at the channel wall.

## Acknowledgements

Experimental work was supported by CNPq – Brazilian Scientific and Technological Council, grants 414216/90-3, 400180/92-8 and 520986/1997-0.

Luís Carlos Demartini thanks CAPES, Ministry of Education, Brazil, for granting him a fellowship.

## References

- Acharya, S., Dutta, S. and Myrum, T. A., 1998. "Heat Transfer in Turbulent Flow Past a Surface-Mounted Two-Dimensional Rib", *Transactions of the ASME*, vol. 120, pp. 724-734.
- Anatoniou, J. and Bergeles, G., 1988. "Development of the Reattached Flow Behind Surface-Mounted Two-Dimensional prisms", *Journal of Fluids Engineering*, vol. 110, pp. 127-133.
- Bergeles, G and Athanassiadis, N., 1983. "The Flow Past a Surface-Mounted Obstacle", *Journal of Fluids Engineering*, vol. 105, pp.461-463.
- Berner, C., Durst, F. And McEligot, D. M., 1984. "Flow Around Baffles", *Journal of Heat Transfer*, vol. 106, pp. 743-749.

De Zilwa, S. R. N., Khezzar, L. K. and Whitelaw, J. H., 1998. "Flows through plane sudden-expansions", *International Journal for Numerical Methods in Fluids*, nr. 32, pp. 313-329.

Demartini, L. C., "Numeric and Experimental Analysis of Pressure and Velocity Fields in a Duct with Baffle Plates", M. Eng. Dissertation, PROMEC/UFRGS, Federal University of Rio Grande do Sul, Porto Alegre-RS, Brazil (in Portuguese)

Endres, L. A. M. 1997. "Experimental analysis of the fluctuating pressure field in tube banks subjected to turbulent cross flow", Dr. Eng. Thesis. PROMEC/UFRGS, Federal University of Rio Grande do Sul, Porto Alegre-RS, Brazil (in Portuguese).

Endres, L. A. M. and Möller, S. V., 2001, "On the fluctuating wall pressure field in tube banks", *Nuclear Engineering and Design*, Vol. 203, pp. 13-26.

Fluent Inc, 2000. "User's Guide 5.2", Centerra Park Lebanon, NH, USA.

Habib, M. A., Mobarak, A. M., Sallak, M. A., Hadi, E. A. A. and Affify, R. I., 1994. "Experimental Investigation of Heat Transfer and Flow Over Baffles of Different Heights", *Journal of Heat Transfer*, vol. 116, pp. 363-368.

Hinze, J. O., 1975. "Turbulence", McGraw-Hill.

Hwang, C. B. And Lin, C. A., 1999. "A low Reynolds number two-equation  $k_\theta$ - $\epsilon_\theta$  model to predict Thermal Fields", *International Journal of Heat and Mass Transfer*, vol. 42, pp. 3217-3230.

Hwang, R. R; Chow, Y. C. and Peng, Y. F., 1999. "Numerical study of turbulent flow over two-dimensional surface-mounted ribs in a channel", *International Journal for Numerical Methods in Fluids*, vol. 37, pp. 767-785.

Kelkar, K. M and Patankar, S. V., 1987. "Numerical Prediction of Flow and Heat Transfer in a Parallel Plate Channel With Staggered Fins", *Journal of Heat Transfer*, vol. 109, pp.25-30.

Launder, B. E. and Spalding, D. B., 1972. "Mathematical Models of Turbulence", Academic Press,

Launder, B. E. And Spalding, D. B., 1974. "The Numerical computation of Turbulent Flows", *Computer Methods in Applied Mechanics and Engineering*, vol. 3, pp. 269-289.

Leonard, B. P. and Mokhtari, S., 1990. "Ultra-Sharp Nonoscillatory Convection Schemes for High-Speed Steady Multidimensional Flow", NASA TM 1-2568, NASA Lewis Research Center.

Li, H. and Kottke, V., 1998. "Effect of baffle spacing on pressure drop and local heat transfer in staggered tube arrangement", *International Journal of Heat and Mass Transfer*, vol. 41, n° 10, pp. 1303-1311.

Möller, S.V., Endres, L. A. M. and Escobar, G., 1999. "Wall Pressure Field in a Tube Bank after a Baffle Plate", *Transactions of SMiRT 15 - 15th International Conference on Structural Mechanics in Reactor Technology*, Vol. 7, pp. 262-275, Seoul.

Patankar, S. V, 1980. "Numerical Heat Transfer and Fluid Flow", Mc Graw-Hill, New York.

Van Doormaal, J. P. and Raithby, G. D., 1985. "Enhancements of the SIMPLE method for predicting incompressible fluid flows", *Numerical Heat Transfer*, vol. 7, pp 147-163.

Wiemer, P., 1937, *Untersuchung über den Zugwiderstand von Wasserrohrkesseln*, Dissertation, RWTH, Aachen.